Available online at www.sciencedirect.com

ScienceDirect

Physica B 393 (2007) 167–174

PHYSICA B

www.elsevier.com/locate/physb

Characteristics of the dielectric relaxation modes of a newly synthesized fluorinated antiferroelectric liquid crystal 6F6B

Geetika Pandey[a,*], R. Dhar[b], V.K. Agrawal[a], R. Dabrowski[c]

[a]Physics Department, Allahabad University, Allahabad 211 002, India
[b]Physics Department, Ewing Christian College, Allahabad 211003, India
[c]Institute of Chemistry, Military University of Technology, 00-908, Warsaw, Poland

Received 23 May 2006; received in revised form 2 September 2006; accepted 1 January 2007

Abstract

The dielectric response of a newly synthesized fluorinated antiferroelectric liquid crystal namely (S) 4-(1-methylheptyloxycarbonyl) biphenyl-4′-yl-4-[6-(tridecafluoro heptanoyloxy)hexan-1-oxy]benzene-1-carboxylate (6F6B) in its planar orientation has been carried out. 6F6B shows a $\mathrm{Cr} \rightarrow \mathrm{SmC}_A^* \leftrightarrow \mathrm{SmC}^* \leftrightarrow \mathrm{SmA}^* \leftrightarrow \mathrm{I}$ phase sequence. It shows five different modes of dielectric relaxations in different phase. In SmA* phase, relaxation frequencies of usual soft mode are temperature dependent and decreases with decrease in the temperature. Dielectric strength is small but increases with decrease in the temperature and follows Curie Weiss' law. Ferro-electric SmC* phase shows Goldstone mode having large dielectric strength in the low-frequency region. Its relaxation frequencies are almost invariant with the temperature. It has been possible to completely suppress Goldstone mode by applying DC bias. Three modes of dielectric relaxation have been clearly observed in antiferro-electric SmC$_A^*$ phase, each of them separated by about two decades of frequency. Two modes are due to the in-phase and anti-phase azimuthal angle fluctuation of the anti tilt pairs of the molecular directors, respectively, whereas the third one is due to ionic conductance, which is common in all phases.

PACS: 61.30.−V; 77.84.Nh; 77.22.Gm; 64.70.Md

Keywords: Antiferroelectric liquid crystal; Dielectric relaxation; Goldstone mode; Soft mode; Ionic conductance

1. Introduction

During the last decade, considerable attention has been given to the potential use of AFLCs in high-resolution flat-panel displays and microdisplays for computers and TVs. Despite the obviously very attractive and well-known electro-optic characteristics of AFLCs, such as the tri-state switching behaviour, easy DC-compensation, fast response (microseconds), easy grey scale and wide viewing angle, there are still no commercial AFLC device available in the market. The main reason for this is the relatively low contrast achieved so far. Most often this has been attributed to the fact that antiferroelectric materials lack a nematic phase. However, there are other reasons behind the bad dark state as well, and those reasons may be even more important. The two factors having the strongest influence are the poor homogeneity of the AFLC bookshelf alignment and the so-called pre-transitional effect [1–3], being a linear response below the threshold for switching from the antiferroelectric to ferroelectric state [4].

In order to solve the poor dark state problem shown by AFLC materials in their antiferroelectric SmC$_A^*$ phase [2,5], efforts have been made to synthesize orthroconic antiferroelectric liquid crystal materials (OAFLC). In OAFLCs, angle between the molecules of two layers of a unit cell of SmC$_A^*$ phase is 90° i.e. tilt of the molecule from the layer normal is 45°. A new group of fluorinated mesogens with $\mathrm{C_nF_{2n+1}COO(CH_2)_3O}$- tail has been recently synthesized [6–8]. These compounds have the smectic layer with anticlinic order (SmC$_A^*$ phase) in broad temperature range and high tilt angle [9]. Before going for electro-optical

---

*Corresponding author. Tel.: +919935667200.
E-mail address: geetika_11@rediffmail.com (G. Pandey).

0921-4526/$ - see front matter © 2007 Elsevier B.V. All rights reserved.
doi:10.1016/j.physb.2007.01.002

studies on these materials it is pertinent to determine different dielectric parameters that are instrumental to control electro-optical properties [10,11]. We have chosen one representative AFLC material (S) 4-(1-methylheptyloxycarbonyl) biphenyl-4′-yl-4-[6-(tridecafluoroheptanoyloxy)hexan-1-oxy]benzene-1-carboxylate (6F6B) from the newly synthesized series and have carried out dielectric spectroscopy. 6F6B has following structure:

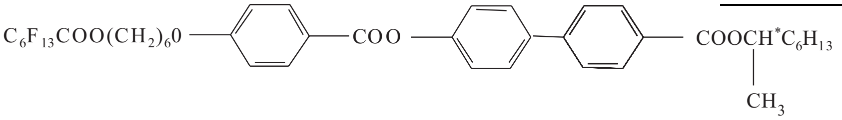

Sample possess para-electric SmA* and ferro-electric SmC* phases beside broad temperature range anti ferroelectric SmC_A^* phase in the vicinity of the room temperature.

2. Experimental techniques

Dielectric studies of the planar aligned sample of thickness 10 μm have been carried out in the frequency range of 1 Hz–10 MHz by using impedance/gain phase analyser of Solartron model SI-1260 coupled with Solartron dielectric interface model-1296. The accuracy in the measurement of capacitance (*C*) and conductance (*G*) in the concerned frequency range is <0.2% and hence maximum uncertainty in the measurement of dielectric permittivity ($\varepsilon'_\perp$) and dielectric loss ($\varepsilon''_\perp$) within the entire frequency range is less than ±1%. The accuracy of measured frequency is ±100 ppm.

Temperature of the sample has been controlled with the help of hot stage of Instec (model HSI-1) with the temperature accuracy of ±0.003 °C. Temperature near the sample has been determined with the help of a copper-constantan thermocouple. A measuring electric field of $0.1\,V_{\rm rms}$ has been applied across the sample in the direction parallel to smectic layers. Dielectric data have been acquired during the cooling cycle. Other details of experimental techniques have already been discussed elsewhere [12].

To analyse the measured data, the dielectric spectra has been fitted with the help of generalized Cole–Cole equation [12,13]:

$$\varepsilon^* = \varepsilon' - j\varepsilon'' = \varepsilon'(\infty) + \sum_i \frac{(\Delta\varepsilon)_i}{1 + (j\omega\tau_i)^{(1-h_i)}} + \frac{A_1}{\omega^n} - j\frac{\sigma(DC)}{\varepsilon_0\omega} - jA\omega^m, \tag{1}$$

where $\varepsilon'(\infty)$ is relative permittivity at high-frequency limit, $\Delta\varepsilon_i$, τ_i and h_i are dielectric strength, the relaxation time (inverse of angular relaxation frequency) and symmetric distribution parameter ($0 \leqslant h_i \leqslant 1$) of *i*th mode, respectively. The third and fourth terms in Eq. (1) represent the contribution of electrode capacitance and ionic conductance at low frequencies where A_1 and *n* are constants [14, 15]. σ(DC) is the ionic conductance and ε_0 (= 8.85 pF/m) is the free space permittivity. The measured dielectric absorption ε'' contains, a spurious contribution above 100 kHz due to finite resistance of ITO coated electrodes [15,16]. An additional imaginary term $A\omega^m$ [15] is added in Eq. (1) to partially account for ITO effect, where *A* and *m* are constants as for as correction terms are small i.e. data are well below reactive cut off frequency [12, 17]. The reactive cut off frequency (f_{x0}) of the cell is given as [17]

$$f_{x0} = f_0\sqrt{\left(1 - \left(\frac{LG^2}{C}\right)\right)}, \tag{2}$$

where *G* and *C* are the AC conductance and capacitance of the dielectric cell filled with the material and $f_0 = 1/2\pi\sqrt{LC}$. *L* is the inductance of the leads connected with the cell. The numerical value of f_{x0} in the present cell is at about 3–10 MHz depending upon the values of C in different phases and therefore correction term is applicable only up to 1 MHz.

The characteristic parameters of all the relaxation modes in different phases have been calculated by fitting Eq. (1) on the experimental data with the help of computer program developed with the help of Origin Software. The results of fitting procedure are shown in Fig. 1.

3. Results and discussion

The temperature dependence of the dielectric permittivity of different phases at various frequencies (see Fig. 2) distinguishes ferroelectric SmC* and anti ferroelectric SmC_A^* phases from para electric SmA* phase. Highest value of $\varepsilon'_\perp$ in SmC* phase (~320) is at 1 Hz. However at such a low frequency there is substantial contribution from electrode polarization effects as well [14,15]. Large variations of $\varepsilon'_\perp$ with frequency in SmC* and SmA* phases are due to the dielectric relaxation modes observed in these phases as can be seen in Fig. 3. High jumps in the values of $\varepsilon'_\perp$ at SmA* to SmC* and at SmC* to SmC_A^* transitions are due to the transformation of paraelectric structure into the ferroelectric structure and ferroelectric structure into the antiferroelectric structure respectively. Fig. 3 shows variations of the relaxation frequencies of different modes observed in different phases. Fig. 4 shows temperature dependence of the dielectric strengths (Δε) for different relaxation modes observed for the material. According to the range of relaxation frequencies and their temperature dependences in different phases, the dielectric relaxation modes are classified into six groups as discussed in coming paragraphs.

In the SmA* phase, relaxation frequency of mode 1 decreases with decrease in temperature (see Fig. 3) and